Chapter 2
Anisotropy of Magnetic Susceptibility

Abstract Anisotropy of magnetic susceptibility is an important technique which depicts preferred orientation of magnetic minerals in a rock or unconsolidated sediments. Hence the property is used for study of primary structures and rock fabric. The technique is non-destructive and can be used in nearly all types of rocks because it does not need a rock to contain specific strain markers like deformed fossils, reduction spots, ooids, etc. The method has an advantage as it can determine weak deformation even where lineation and foliation have not developed. In rocks with well developed tectonic fabrics, the principal magnetic susceptibility directions are closely related to orientation of structural features (e.g. fold, fault, foliation, lineation). Different types of AMS fabrics are described. Differences between magnetic and petrofabric strains are highlighted. Importance of sampling in a region of superimposed deformation is described. It is emphasized that objectives of the study should be formulated prior to selection of sample sites. Hrouda diagram is described for understanding the roles of simple and pure shear deformations in a region of simultaneous development of folding and thrusting. The technique has been successfully employed to ascertain the displacement patterns along some of the prominent Lower Himalayan thrusts.

When a magnetic field is applied on a rock sample, the intensity of magnetization is not always uniform in all directions but varies with orientation of the constituent minerals. Hence the property can be used for study of rock fabric. The dependency of induced magnetization on orientation of the applied magnetic field in a rock is called as anisotropy of magnetic susceptibility (AMS) and it depicts the preferred orientation of magnetic minerals in a rock or unconsolidated sediments (Hrouda 1982, Tarling and Hrouda 1993). The first systematic study in this field was performed by Voight and Kinoshita (1907). It was later used as a petrofabric marker by Ising (1942) and Graham (1954). The technique is non-destructive and does not need a rock to contain specific strain markers like deformed fossils, reduction spots, ooids etc. Hence it can be used in nearly all types of rocks. The method has an advantage as it can determine weak deformation even where lineation and foliation have not developed (Tarling and Hrouda 1993; Borradaile and Henry 1997; Evans et al. 2003).

A. K. Dubey, *Understanding an Orogenic Belt*, Springer Geology,
DOI: 10.1007/978-3-319-05588-6_2,

In rocks with well developed tectonic fabrics, the principal magnetic susceptibility directions are closely related to orientation of structural features (e.g. folds, faults, foliation, lineation) (Hrouda and Janak 1976; Borradaile 1988; Averbuch et al. 1992; Robion et al. 2007; Borradaile and Jackson 2010). Some of the important aspects of the technique are described here (details in Tarling and Hrouda 1993).

2.1 Different Forms of Magnetization

The technique can be applied to rocks even where the magnetic minerals are absent because the magnetic properties arise from motion of electrically charged particles. When electron shells are complete (even atomic numbers) in a substance, application of a magnetic field results in electron spin and generate magnetization. The strength of magnetization is measured in different orientations and the difference is then interpreted in terms of net shape of the grains or degree of their crystalline alignment (petrofabric). Depending on the nature of this magnetization and the magnetization when the field is removed, different forms of magnetization can be identified.

A material is called as diamagnetic when the generated magnetization is in opposite direction to that of the applied field and it is lost immediately after removal of the external magnetizing field (Fig. 2.1a). Since the field is produced in opposite direction to that of the applied field, the diamagnetic substances have negative susceptibilities (~10^{-5} SI) for common rock forming minerals (e.g. quartz, calcite, dolomite). All other substances, with incomplete electron shells, are described as paramagnetic (Fig. 2.1b). These substances are characterized by a magnetic moment that follows the direction of the applied field. The paramagnetism also disappears immediately after removal of the applied field. Paramagnetic minerals have positive susceptibilities that range between 10^{-2} and 10^{-4} SI for common rock forming minerals (e.g. hornblende, chlorite, biotite, muscovite, tourmaline).

A few substances with strong positive susceptibilities can also carry a strong ramanent magnetization (magnetization that remains after the external magnetizing field has been removed). These substances are called as ferromagnetic or loosely as magnetic (Fig. 2.1c). Ferromagnetism is characteristic of substances in which magnetic vectors and the applied field are in the same direction and retain their magnetic alignment after removal of the field (e.g. magnetite, haematite). These materials acquire and retain a very strong magnetism that is superposed on paramagnetic character. Thus if the ferromagnetic properties are destroyed (e.g. by heating), the previously ferromagnetic materials behave as paramagnetic. When the two lattices are strongly magnetized in equal amount, the mineral grains will have no net magnetization resulting in antiferromagnetic substances (e.g. haematite) (Fig. 2.1d) and are characterized by a sub-division in their lattices (designated as A and B sub-lattices). The atomic moments of A and B are aligned antiparallel to each other. Hence when the magnetic moments are equal, they cancel each other and the resultant magnetic moment is nil. When, the lattice is more strongly

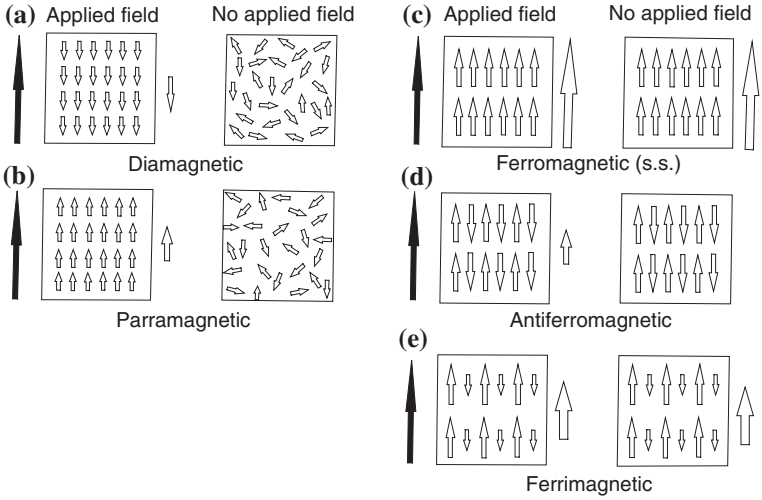

Fig. 2.1 Different forms of magnetization. The *left hand* diagrams in the pairs of illustrations 'a' to 'e' show the magnetization (*hollow arrow outside the square*) that a substance acquires in an applied magnetic field (*solid arrow*). The *right hand* diagrams depict the magnetization present after the field has been removed. **a** Diamagnetic materials become weakly magnetized in opposite direction to that of the applied field, but electron spins randomly on removal of the field. **b** Paramagnetic materials (e.g. olivine, pyroxene) become weakly magnetized in the same direction as that of the applied field, but randomize on its removal. (**c**), (**d**) and (**e**) Ferromagnetic materials retain their magnetic alignment after removal of the field. **c** Ferromagnetic materials acquire and retain a very strong magnetization. **d** The magnetic alignments of antiferromagnetic materials are exactly anti-parallel and most paramagnetic effects are completely dominated by these very strong internal fields. These materials have no external magnetic field after removal of the applied field. **e** The alignments within ferromagnetic materials are antiparallel but not of equal magnitude, so they retain a weaker external magnetization than a ferromagnetic material when the applied field is removed [From Tarling and Hrouda (1993), © D. H. Tarling. Published with permission of D. H. Tarling]

magnetized resulting in weak net magnetic field (e.g. magnetite) the substances are called as ferrimagnetic (Fig. 2.1e). These substances have unequal atomic moments in their sub-lattices and a net spontaneous magnetization, which gives rise to a weak ferromagnetism (Dunlop and Ozdemir 1997). The antiferromagnetic and ferrimagnetic are together referred as ferromagnetic.

2.2 Anisotropy of Magnetic Susceptibility

A natural rock contains a variety of minerals with ferromagnetic, paramagnetic, or diamagnetic properties. Depending on the magnetic properties, each grain contributes to the total (bulk) susceptibility and its anisotropy. When ferromagnetic minerals exceed 0.1 volume percentage of the whole rock, they control the magnetic

properties. In absence of these minerals, the susceptibility of paramagnetic minerals tends to dominate the diamagnetic minerals provided they constitute more than 1 % of the rock.

The susceptibility also depends on temperature and strength of the applied field. Since these are not constant features, the measurements are normally done at room temperature [~20 °C at magnetic fields of <1 mT (milli Tesla)].

The magnitude of anisotropy of magnetic susceptibility, determined from measurements of susceptibility in a weak field, depends on two factors; (i) anisotropy of particles themselves, and (ii) degree of their alignment. The individual particles may represent crystalline or shape anisotropy. The crystalline anisotropy depends upon action of lattice forces and resulting magnetization along specific directions, e.g. a crystalline axis or plane, termed as easy axis or easy plane. In shape anisotropy, the induced magnetization is normally oriented along the long axis of the grains. The ratio of crystalline and shape anisotropies varies in different minerals. For example, in magnetite, the crystalline anisotropy is weak and the shape anisotropy is dominant. In a special condition when crystalline 'easy' axes and long (shape) axes of the grains have the same orientation, the magnetic anisotropy of the rock is maximum.

When strength of induced magnetization per unit volume is directly proportional to strength of the applied magnetic field, it can be represented as:

$$M \alpha H$$
$$M = KH$$
$$K = M/H$$

where,

M Strength of the induced magnetization per unit volume
K Constant of proportionality defined as magnetic susceptibility of the material, and
H Strength of the applied magnetic field

Any difference in magnetic strength of the constituent minerals can be deduced in terms of net shape of the grains and degree of their crystalline alignment. This can be interpreted in the same way as other petrofabric techniques normally employed in structural geology (Tarling and Hrouda 1993; Borradaile and Henry 1997; Evans et al. 2003).

2.3 Equipment

Directional susceptibility of rocks is generally measured by low field bulk susceptibility (details in Tarling and Hrouda 1993). Anisotropy of a sample is determined by measurement of magnitude of susceptibility along at least six directions so that the susceptibility ellipsoid can be drawn. A common type

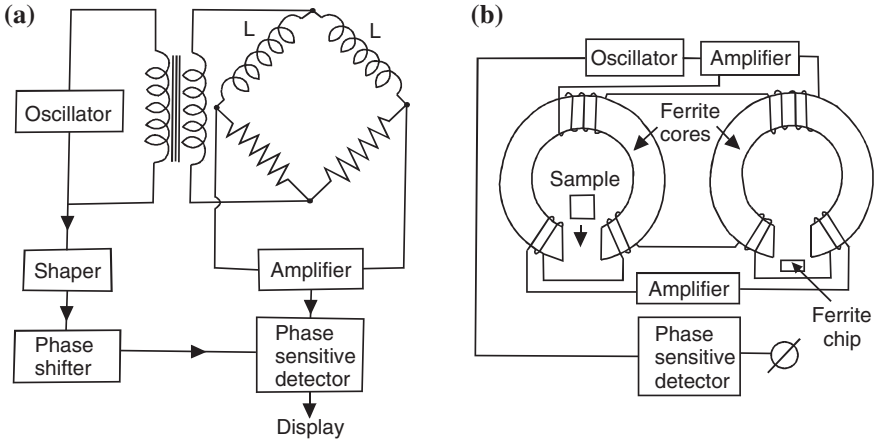

Fig. 2.2 Directional susceptibility meters. Two bridge systems for determination of magnetic susceptibility along the direction of a coil. **a** An equal-impedance bridge. The specimen can be inserted into one of the coils (*L*). **b** The balanced-transformer system where the specimen is placed inside a ferrite ring. The extent of unbalancing the circuit is proportional to susceptibility of the specimen in the direction of circumference of the ring [From Tarling and Hrouda (1993), © D. H. Tarling. Published with permission of D. H. Tarling]

of instrument is a modified a.c. bridge, one arm of which is an inductive coil (Fig. 2.2a). When a rock sample is placed in the coil, the change in inductance of the coil is proportional to the sample susceptibility. Initial calibration is normally done by using a specimen holder containing a known volume of a salt of known susceptibility (e.g. copper sulphate). Subsequent calibrations are performed with a strip of recording tape (meghamite) whose susceptibility has been measured by using the salt sample.

In the balanced-transformer equipment (Fig. 2.2b), a sample is surrounded by one of the sensing coils. Insertion of the sample alters the mutual inductance between the two coils producing a net output voltage in an associated circuit.

The specimen's susceptibility is measured in 15 orientations using a rotatable case. From these values six independent components of susceptibility tensor and statistical errors are calculated using the SUSAM software.

2.4 Collection of Samples

AMS studies require carefully chosen oriented rock samples. These should be fresh i.e. free from weathering and solution activities. In presence of prominent cleavage or thin bedding, the sample is likely to split during drilling. On the other hand, if the rock is hard and massive, it is difficult to extract an oriented sample. Hence a field geologist, who intends to do AMS (and petrofabric strain) studies,

should always carry a light and a heavy hammer, set of chisels, nylon and wire brushes (to wipe a sample for necessary markings prior to its extraction), and a small sprit level for marking the horizontal plane.

Prior to extraction of a sample, the rock surface is marked for strike and dip directions, amounts, and an upright arrow. Structural data (e.g. bedding, flow indicators, lineation, foliation, minor faults) are measured and recorded in a field note book along with the location. The structural data should be recorded as close to the sample as possible, especially in areas of superimposed deformation. Each sample is given a distinct name and number. Since a good number of drill cores (5–10) are required for analysis, it is advisable to collect large samples ($\geq 15 \times 10 \times 5$ cm). The samples are brought to laboratory and fixed firmly in its natural orientation either by using cement or by clamping by a set of vices. The samples are then drilled, cores are taken out and cut to the required size. In an ideal situation, each specimen for anisotropic studies should be a sphere but it is not convenient to cut an oriented sphere from a rock specimen. Hence two most common standard shapes are cylinders with a diameter of 2.5 cm and height of 2.1 cm, and cubes of 2.0 cm side (Tarling and Hrouda 1993). Cubes are normally cut in semiconsolidated sediments. Portable drilling machine are available for obtaining drill cores in field but the machine requires a continuous supply of water or lubricant. This is not very convenient because it is difficult to carry large quantities of water/lubricant while tracking or climbing a mountain. Proper care should be taken for safe transit of the samples although it is possible to reassemble broken samples by using non-magnetic fast setting epoxy glues. The nonmagnetic property of the glue must be tested before its application because many of the glues are quite strongly magnetic when set.

Soft samples are collected by pushing a plastic cylinder (normally a diameter of 55 mm) or box (sides 2.0–2.1 cm) into sediments. Copper or brass tubes can be used for comparatively harder sediments. The orientations are marked on the body of the container and the required length is later cut in laboratory. Unconsolidated lake sediments or marine sequences are sampled with coring devices that penetrate the surface by gravity loading or with the help of hydraulic pressure. The gravity corers consist of nonmagnetic materials like aluminium. The sediment core is then preserved inside a properly sealed plastic tube for transportation. The sealing is an important part of sampling as drying of the sample can alter the properties. The bulk susceptibility of sediments can be measured by using long core devices but in order to determine the anisotropy of susceptibility, the samples need to be tailored to the required size of the equipment container. Special care should be taken to check the geometry of the tube or box as asymmetric shapes can induce significant error in measurements. The samples should ideally be stored at 2–3 °C to avoid any physical (shape) or chemical changes and the analysis should be performed as early as possible. Samples with high water content can deform during sampling (while pushing the sample tube or box). However this deformation is confined near the walls of the container and bulk of the sample contains the original fabric. This can also be avoided by using cylinders of large diameter so that the peripheries

can be cut and removed prior to the measurements. Some of the soft samples can acquire a fabric, which is oriented along the pushing direction of the cylinder. In order to preserve orientation marks on friable rocks, the marks are made on a flat plastic or wood disc glued to the sample (normally top of the sample).

2.4.1 Importance of Sampling in an Area

The deformation pattern is unlikely to be distributed uniformly in a region and part of the region (sample site) may show only a part of the structure. This is further exemplified by using a deformed modeling clay layer surface (Fig. 2.3a). The multilayer model was deformed in two horizontal directions during successive stages of deformation. The first compression resulted in displacement along the thrust and early folds. The second compression was orthogonal to the early axis of maximum compressive stress, and it formed superposed folds, extensional faults and a strike-slip fault. Selection of sample sites is very important in such a region. A sample collected at site 1 (in vicinity of a thrust; Fig. 2.3b) will reveal the thrust related strain pattern. Sample site 2 is located on an early antiformal hinge related to the early deformation. A sample collected at site 3 is likely to show a reversal of the axes of maximum and minimum compression as compared to site 2 because of the superposed deformation. Site 4 is located near an extensional fault hence this will exhibit maximum compression axis in the vertical direction and the minimum compression in the horizontal direction. On the contrary, site 5 (strike-slip fault) will show the maximum and minimum compression axes in two horizontal directions. Site 6 is located at a distance from all the dominant structures hence this site will reveal the minimum strain values. These variations will be reflected in orientations of developing foliation, lineation, etc. and the magnetic susceptibility. Hence minor structures in close vicinity of the sample site should be carefully recorded and a correlation between orientation of susceptibility axes and strain should not be assumed but established.

Location of sample sites is also important in regions, which have undergone a single phase of deformation because geological structures initiate from a point and then propagate with progressive deformation (details in Chap. 3). Strain values can vary along a thrust, across a thrust, in different fold geometries, and even in two limbs of a fold. The values will be different in thin and thick layers of a single fold, in overturned fold limbs, in an earlier formed fold of a single fold complex, and at the culmination point of a fold surface. Hence the purpose of strain determination should be clear in mind before initiating the study. For example, whether the study is for understanding fold interference patterns, propagation of a fault, strain variation along or across a shear zone or across fold limbs. It is suggested that an area where strain studies are to be performed should be carefully mapped for geological structures and their geometries. This should be followed by selection of sample sites keeping in view the objectives of the study.

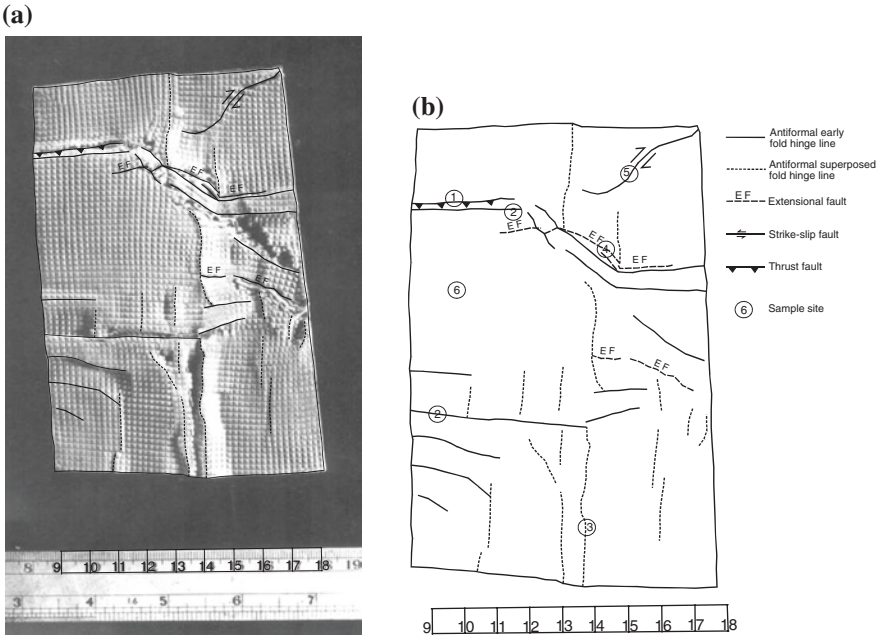

Fig. 2.3 **a** A deformed layer surface after 11 % total model shortening in the first phase and 17 % shortening in the second phase of superposed deformation when the axis of maximum compression was orthogonal to the first axis of maximum compression. A square grid pattern was embossed on the layer surface prior to the deformation. The deformed grids reveal that the surface strain pattern is not uniform throughout the layer. **b** Structural features and sample sites observed on the layer

2.5 Magnetic Anisotropy

When strength of magnetization depends on sample orientation within a magnetic field and the susceptibility varies in different directions, the rock is called as magnetically anisotropic. In anisotropic rocks, the magnetic susceptibility can be represented as a second order symmetric tensor that can be represented geometrically as an ellipsoid with three principle susceptibility axes. The maximum susceptibility is designated as K1, the intermediate as K2, and the minimum as K3 (Kmax > Kint > Kmin). The intensity of these parameters can also vary with relative proportions of ferromagnetic and paramagnetic minerals in the specimen.

Different minerals are characterized by different anisotropies. For example, the crystalline anisotropy is weak in magnetite and the shape anisotropy is dominant whereas in hematite the crystalline anisotropy is dominant. Because of their strong magnetic properties, the ferro- and ferromagnetic minerals are important for magnetic susceptibility studies but in weakly metamorphosed rocks and sediments, the paramagnetic minerals control the AMS (Rochette 1987; Pares 2004).

2.5.1 Mean Susceptibility (Km)

AMS measures the bulk-preferred orientation of ferromagnetic, paramagnetic, and diamagnetic minerals and/or crystal lattices (Hrouda 1982). When the induced magnetization has equal strength in all directions, the rock sample is magnetically isotropic. The mean (average) susceptibility (Kmean) of a specimen is mean value of the directional susceptibilities and is given by:

$$\text{Kmean} = \frac{\text{K1} + \text{K2} + \text{K3}}{3}$$

Another important parameter, normalized anisotropy degree (H) is obtained as follows.

$$\text{H} = \text{K1} - \text{K3}/\text{Kmean}$$

2.5.2 Magnitude of Anisotropy

The anisotropy degree (P or P2) is ratio of the maximum and minimum susceptibilities, i.e.

$$\text{P} = \text{P2} = \text{K1}/\text{K3}$$

The eccentricity of an ellipsoid can also be expressed in terms of axial ratios as follows.

P1 = K1/K2 (the ratio is also known as lineation, L)
P3 = K2/K3 (the ratio is also known as foliation, F)

It is generally accepted that in regions of strong deformation, magnetic lineation is parallel to extension direction (Kmax) and orientation of Kmin axis is parallel to shortening direction (Borradaile and Henry 1997; Housen et al. 1996; Sagnotti et al. 1994; Pares et al. 1999).

Orientation of the susceptibility ellipsoid can be determined precisely in three dimensions and orientation of the susceptibility axes can be used to infer the primary lineations (e.g. flow direction in sediments, emplacement directions in intrusive and extrusive rocks). AMS is particularly useful in characterizing soft sediment deformation (Schwehr and Tauxe 2003) as it can unravel the susceptibility ellipsoid orientation in weakly deformed sediments and rocks, where tectonic fabric has not developed (Borradaile and Henry 1997; Pares 2004). Hence the study has been used extensively for Quaternary deformation and seismotectonic studies (Sagnotti and Speranza 1993; Housen et al. 1996; Sagnotti et al. 1998; Pares et al. 1999; Lee and Angelier 2000, Borradaile and Hamilton 2004, Levi et al. 2005). These studies demonstrate that AMS is an effective tool to distinguish components of sedimentary fabric (resulting from compaction) and earthquake induced structures. Levi et al. (2006) have analyzed sedimentary and seismic origin of clastic dikes in the

Dead Sea Basin and observed that AMS can be very well used for paleoseismic records. AMS has also helped in unraveling coseismic faulting in a trenched fault zone in late Holocene sediments (Jayangondaperumal et al. 2010).

2.6 Different Types of AMS Fabrics

AMS studies in different tectonic settings and particularly in fold-and-thrust belts have described three major categories of AMS fabric types based on relationship between bedding plane and magnetic foliation plane (Sagnotti et al. 1998; Pares et al. 1999; Saint-Bezar et al. 2002; Pares 2004; Robion et al. 2007). Type 1 pattern is essentially sedimentary where the bedding and magnetic foliation are parallel with weak development of magnetic lineation. Type 2 pattern is characterized by magnetic lineation normal to shortening direction and parallel to fold hinge line while the magnetic foliation is parallel to bedding. This is also referred to as mixture of sedimentary and tectonic fabrics (Borradaile and Tarling 1981; Kissel et al. 1986). In type 3 pattern, magnetic lineation is developed perpendicular to shortening direction and bedding plane makes an angle with magnetic foliation plane (Borradaile and Henry 1997).

Later, Robion et al. (2007) have suggested six types of fabric patterns (type 1 to type VI). The sedimentary and tectonic fabrics were differentiated by the angle between mean K3 axes and pole to bedding. Type I and II are sedimentary fabric where K3 is parallel to bedding pole or the angle between K3 and the bedding pole varies from 0° to 15°. Type III corresponds to an intermediate fabric in which K3 is parallel or oblique to bedding (15°–75°). However scattering of K3 around bedding plane may indicate overprinting of tectonic fabrics. When K3 lies within bedding plane, and angle between K3 and bedding pole is greater than 75°, the fabric is described as type IV or cleavage fabric (Pares 2004). Types V and VI are characterized by scattering of K1 around K3 or well grouping of the two, normal to bedding plane. It is to be noted that in all AMS studies, especially in fold-and-thrust belts, sedimentary fabric pattern progressively change to tectonic fabric (Kissel et al. 1986; Housen and van der Pluijm 1991; Aubourg et al. 1995; Pares et al. 1999).

2.7 Plotting of Magnitude and Shape of Susceptibility Ellipsoid

Chapter 1 describes the three-dimensional plot of strain ellipsoid on a two dimensional Flinn diagram. Conceptually, plotting of the susceptibility ellipsoid shapes and their magnitudes is not much different from the Flinn plot. The axial ratios of a magnetic ellipsoid are plotted in the susceptibility plot with foliation (F = K2/K3) along the horizontal axis and lineation (L = K1/K2) along the

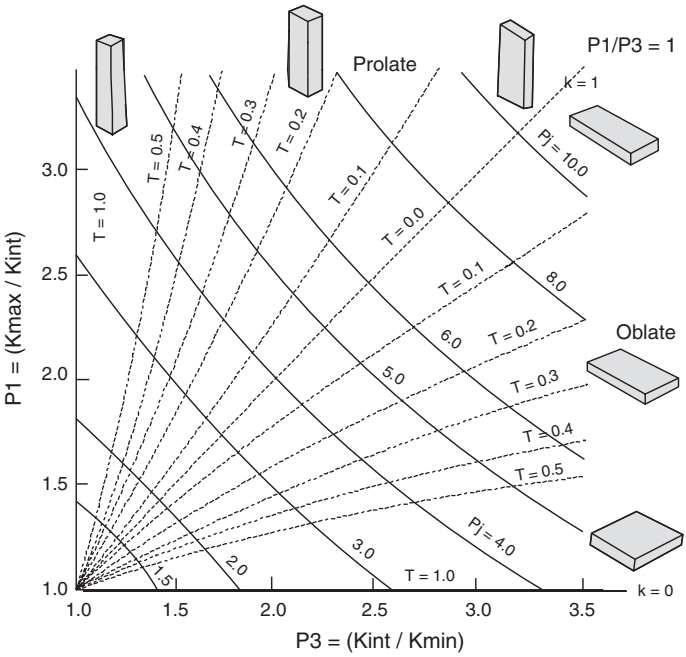

Fig. 2.4 Shapes of AMS ellipsoids in terms of anisotropy degree (Pj) [From Tarling and Hrouda (1993), © D. H. Tarling. Published with permission of D. H. Tarling]

vertical axis (Fig. 2.4). The 45° slope represents the plane strain (triaxial) ellipsoids and divides the area of oblate (disc shape) strain in the lower part and prolate (cigar shape) strain in the upper part. All the ellipsoids with increasing axial ratios plot at increasing distance from the origin.

The technique can provide some help in differentiating the fabrics developed during lithogenesis or during a subsequent tectonic event. For example, depositional or compactional loading normally results in oblate ellipsoid whereas a sheath fold (Chap. 3) reflects a prolate ellipsoid. The diagram also helps in correlation of magnetic and tectonic strains.

In case of unconsolidated sediments the following shape parameter (q) is used.

$$q = \frac{K1 - K2}{K1 + K2/2} - K3$$

The fabric is oblate when $q < 0.69$ and prolate when $q > 0.69$

The shape parameter (T) combines the lineation and foliation parameters to provide a single measure of both properties as follows.

$$T = (\ln L - \ln F/(\ln L + \ln F)$$

The shape parameter (T) has an advantage because it includes all the three principal susceptibilities in its calculation and is symmetrical in its distribution of

values over the full range of ellipsoid shapes. Oblate (disc) shape corresponds to $0 < T \leq 1$, whereas negative values, $-1 \leq T < 0$ correspond to prolate (cigar or rod) shapes (Fig. 2.4). For neutral (plane-strain) ellipsoids, $T = 0$.

The corrected anisotropy degree (Pj) (Jelinek 1981) is intrinsic anisotropy, which either reflects the degree of alignment of minerals as a function of strain intensity or magnetic mineralogy that is linear to bulk susceptibility (Km) (Borradaile 1988; Pares and van der Pluijm 2002).

The parameter can be obtained as follows.

$$\text{Ln (Pj)} = \sqrt{2((\ln K_{MAX}/k))^2 + (\ln(K_{INT}/k))^2 + (\ln(K_{MIN}/k))^2)^{1/2}}$$

The parameter Pj is based on logarithmic values of susceptibility, which are more appropriate in view of lognormal distribution of this property. Most importantly, it incorporates both the intermediate and mean susceptibilities rather than just the maximum and minimum values hence this is a more informative parameter as compared to P_2 alone.

2.7.1 Jelinek Plot (Shape Plot)

This is another two-dimensional plot for depicting the magnitude and shape of susceptibility ellipsoids where the parameters Pj and T are used (Fig. 2.5; Jelinek 1981). Pj is plotted along the horizontal axis ($1 < Pj$) and the shape parameter (T) is plotted along the vertical axis ($-1 < T < 1$). All the prolate shapes have negative values, the triaxial (plane strain ellipsoid) shapes have zero value, and the oblate shapes have positive values tending towards 1.0. Hence both magnitudes and shapes are revealed as the values are plotted linearly with distance. Thus ellipsoid pattern in an area can be observed at a glance.

In some of the minerals (e.g. tourmaline), the longer crystallographic axis (c-axis) corresponds to K3. The property is known as inverse anisotropy and such minerals cannot be used for plotting the AMS ellipsoid.

Shape of the AMS and strain ellipsoids are described in the same way as follows.

Oblate $x = y > z$
Neutral $x/y = y/z$
Prolate $x > y = z$

The above concept appears to be similar to finite strain ellipsoid but the two ellipsoids differ in the following aspects (Borradaile and Jackson 2010).

The strain ellipsoid is dimensionless (i.e. of unit volume) but represents the shapes of strained objects and quantifies these in form of an ellipsoid which can be compared in different outcrops. Strain estimation using a deformed object of known shape provides accurate measurement of strain but this strain value is representative of the object, and not of the entire rock. The matrix and the object may have undergone different amounts of shortenings depending on their rheological

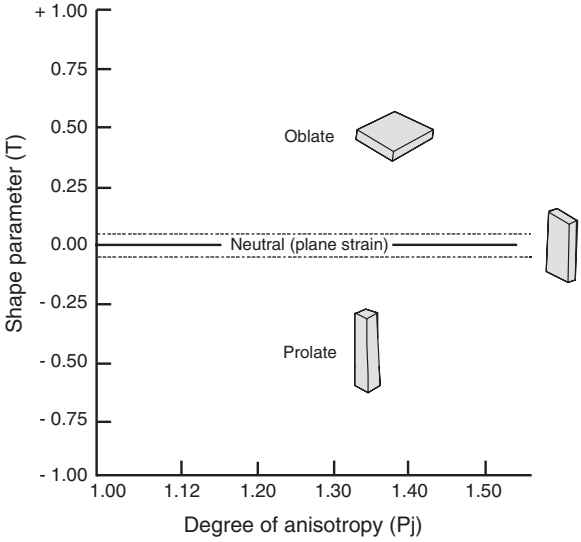

Fig. 2.5 Jelinek plot showing the relationship between degree of anisotropy, Pj, and shape parameter, T [From Tarling and Hrouda (1993), © D. H. Tarling. Published with permission of D. H. Tarling]

properties. Similarly, finite strain determined from fold shapes (unfolding of ptygmatic folds or flattened parallel folds) provide the maximum strain when measurements are made on the maximum amplitude fold with lowest interlimb angle in a competent layer. Adjacent folds with comparatively larger interlimb angles reveal lower strain values. It is also to be noted that layers of the same competence may reveal different finite strain values as a result of variation in fold geometries across a multilayer fold profile and variation in the ratio of layer parallel to buckle strain. Additional complications arise because of three-dimensional variations in fold shapes and superimposed folding (Chap. 3). On the contrary, magnitudes of AMS ellipsoids are the result of different mineral assemblages in the rock samples. Hence the AMS ellipsoid represents the anisotropy of a physical property and the mean susceptibility reveals relative AMS for different specimens obtained from different outcrops. The AMS ellipsoid is a fabric ellipsoid, which may not directly relate to strain. It should be regarded as a petrofabric tool which represents orientation distribution of all minerals and all sub-fabrics in a specimen. Magnitudes of the ellipsoid axes are properties of the state of matter and it can vary in shape and magnitude because different specimens can differ in mean susceptibility (k). However the AMS ellipsoid has an advantage over the finite (petrofabric) strain ellipsoid because it can isolate the sedimentary (depositional), tectonic, and overprint tectonic fabrics. The AMS ellipsoid combines the influence of all minerals forming the sample although the most abundant, high-k, and strongly anisotropic minerals control the rock AMS. For example, high susceptibility of the common oxides (e.g. magnetite) and sulphides of iron (e.g. pyrite) are of special significance. Some of the rocks (e.g. quartzite, limestone, tonalite, rhyolite) may reveal very low susceptibilities ($k \sim 0$ or $k < 0$ along some axes) thereby making it impossible to draw a magnitude ellipsoid. Since a rock is an aggregate

of different minerals with variable properties, for a successful AMS analysis, a sample should be sufficiently homogeneous and the grain size should not be very large. Hence the AMS ellipsoid depends on the mineral abundances and different mineral AMS (Borradaile and Jackson 2010). Further, the AMS ellipsoids can vary in shape and magnitude because of different mean susceptibility (k) in different specimens.

The AMS principal directions can be used to obtain stress and finite-strain directions from weakly deformed rocks at low temperatures. However, shape of the strain ellipsoid (magnitude of strain) is difficult to obtain because strong preferred orientations produced by stress-controlled crystallization have a maximum AMS that cannot increase with strain (Borradaile and Henry 1997). Additional problems arise at low and strong deformations. For a valid correlation between AMS magnitudes and strain it is essential that the maximum shortening is >30 % so that primary AMS fabrics (e.g. compaction during sedimentation) are obliterated. In regions of intense deformation, where the shortening is ~70 %, the mineral alignments are saturated and Pj acquires a plateau. Moreover, there are certain strain markers that are larger than the standard AMS core (e.g. lava pillows, pebbles, xenoliths, etc.). These markers reveal the grain strain and alignment but the inter-granular motion cannot be detected by AMS. These features demand that in order to have a better comparison, the same sample should be used for AMS and strain measurements because the proportions of constituent magnetic minerals may differ in different samples. The finite strain indicators reveal a sum of several increments of strain that may have acted in different directions. Thus it is possible to identify the principal strain directions but it is difficult to predict any systematic angular relationship to principal stress directions during progressive deformation (Borradaile and Henry 1997).

Anisotropy of susceptibility is controlled by crystallographic orientations of the mineral grains but is not affected by grain shape. It is also to be noted that AMS axes and crystal axes rarely show a one-to-one correspondence (Borradaile 1988). The magnitude of strain is normally less in AMS as compared to the strain.

2.7.2 Plotting of the Principal Axes

Directions of the principal axes of susceptibility ellipsoids can be plotted on equal area or equal angle stereographic projections. However, keeping the uniformity of structural plots of field data (bedding, field lineations, field foliations etc.), structural geologists prefer the lower hemisphere, equal area plots. This helps in plotting of field and magnetic data on one diagram for a quick comparison between the two. The axes of maximum, intermediate and minimum susceptibility are plotted as squares, triangles and circles, respectively (Fig. 2.6). As a normal practice all points plotted in the lower hemisphere are solid symbols but hollow, if plotted on the upper hemisphere. The minerals crystallizing in orthorhombic and tetragonal systems are easy to interpret because principal susceptibilities and crystal axes are generally

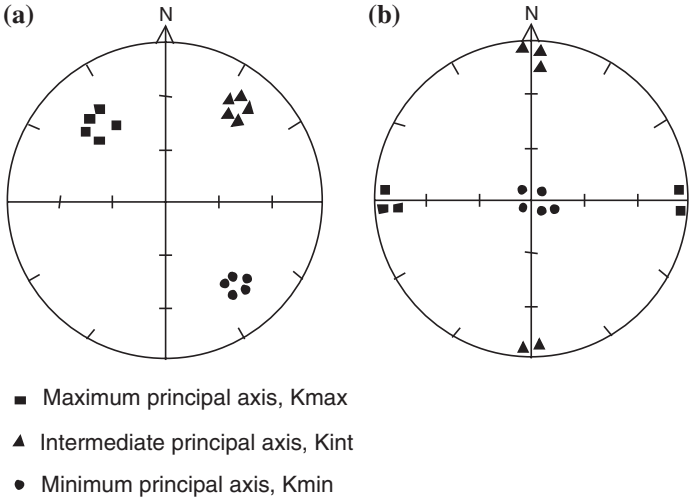

Fig. 2.6 Plotting of the three principal susceptibility axes on lower hemisphere of the equal area net. **a** All the three axes are inclined. **b** The minimum principal axis is vertical whereas the other two are horizontal

parallel. However most of the rock forming silicates are monoclinic in which only one axis corresponds to one of the principal susceptibilities. The triclinic minerals are more complicated because no susceptibility axis is parallel to a crystal axis. The precise orientations of susceptibility axes with respect to crystal axes are yet to be understood completely (Borradaile and Jackson 2010).

2.8 Hrouda Diagram

The Hrouda diagram is based on the property that platy minerals rotate and align during deformation. Initially the minerals may have random orientation (Fig. 2.7a) but with increase in simple shear, the minerals rotate and align parallel to the shear direction thereby producing a preferred orientation (Fig. 2.7b).

Thrusting in orogenic belts involves a combination of pure- and simple-shear mechanisms. The simple-shear is regarded as lying on the thrust surface and parallel to the direction of displacement under the plane-strain condition. The constituent minerals rotate and tend to align parallel to the thrust surface. The degree of alignment of minerals is proportional to magnitude of the simple shear. After the alignment, the minerals have a nearly uniform angular relationship with the thrust surface, which is normally the bedding (flat thrust). Hence a relationship can be established between orientation of constituent platy minerals (magnetic foliation), bedding and other parameters related to deformation. One such relationship was proposed by Hrouda (1991) in which angle (f) between bedding and magnetic

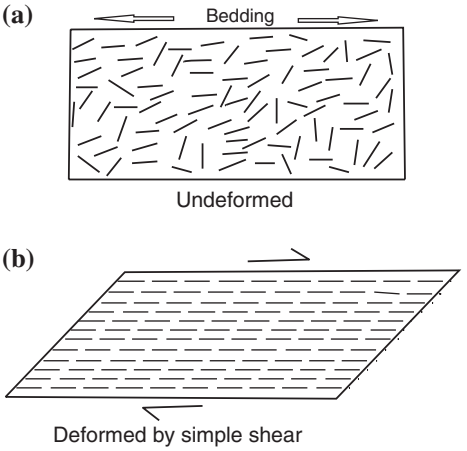

Fig. 2.7 Reorientation of platy minerals during simple shear. **a** Random orientation of platy minerals prior to deformation. **b** Alignment of the minerals parallel to the shear direction

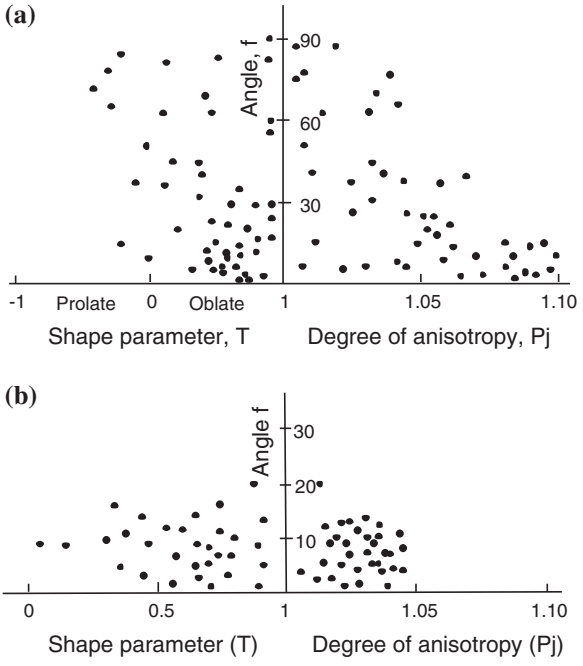

Fig. 2.8 Hrouda diagram illustrating relationships of angle between bedding and magnetic foliation, degree of anisotropy and shape parameter. **a** Weak deformation. **b** Strong deformation

foliation was plotted along the vertical axis whereas the degree of anisotropy (Pj), and shape parameter (T, oblate to plane strain to prolate) were plotted along the horizontal axis (Fig. 2.8). At the outset of deformation, the platy minerals display a random orientation and their angle with the bedding may vary from 0° to 90° (Fig. 2.8a). At large deformations, bedding and magnetic foliation tend to acquire parallelism (i.e. decreasing angle f) (Fig. 2.8b). Hence distribution pattern of different

sites can indicate the extent of deformation. The shape parameter and degree of anisotropy, though not conclusive, can suggest the intensity of deformation. A large variation of 'f' in a strongly deformed rock sequence normally indicates pure shear deformation with a large number of smaller folds.

The diagram is effective in evaluating the extent of simple shear in an area, which has undergone thrusting. However complications may arise in areas of superimposed deformation. Superposed folds (later formed folds) have their own geometries and these can affect the early relationship between bedding and foliation. In such areas it is advisable to ignore locations of superposed folds while collecting samples for construction of the diagram. The samples must be at a safe distance from superposed folds where the effect of superposed strain is minimal.

References

Aubourg C, Rochette P, Bergmuller F (1995) Composite magnetic fabric in weakly deformed black shales. Tectonophysics 87:267–278

Averbuch O, Lamotte DF, Kissel C (1992) Magnetic fabric as a structural indicator of the deformation path within a fold-thrust structure: a test case from the Corbieres (NE Pyrenees, France). J Struct Geol 14:461–474

Borradaile GJ, Hamilton T (2004) Magnetic fabrics may proxy as neotectonic stress trajectories, Polis rift, Cyprus. Tectonics 23(TC1001):1–11. doi:10.1029/2002TC001434

Borradaile GJ, Henry B (1997) Tectonic applications of magnetic susceptibility and its anisotropy. Earth Sci Rev 42:49–93

Borradaile GJ, Jackson M (2010) Structural geology, petrofabrics and magnetic fabrics (AMS, AARM, AIRM). J Struct Geol 32:1519–1551

Borradaile GJ, Tarling DH (1981) The influence of deformation mechanisms on magnetic fabric in weakly deformed rocks. Tectonophysics 77:151–168

Borradaile GJ (1988) Magnetic susceptibility, petrofabrics and strain. Tectonophysics 156:1–20

Dunlop D, Ozdemir O (1997) Rock magnetism, fundamentals and frontiers. Cambridge Studies in Magnetism, Cambridge University Press, Cambridge, p 272

Evans MA, Lewchuk MT, Elmore RD (2003) Strain partitioning of deformation mechanism in limestones: Examining the relationship of strain and anisotropy of magnetic susceptibility (AMS). J Struct Geol 25:1525–1549

Graham JW (1954) Magnetic susceptibility anisotropy, an unexploited petrofabric element. Geol Soc Am Bull 65:1257–1258

Housen BA, van der Pluijm BA (1991) Slaty cleavage development and magnetic anisotropy fabrics (AMS and ARMA). J Geophys Res 96:9937–9946

Housen BA, Tobin HJ, Labaume P, Leitch EC, Maltman AJ, Ocean Drilling Program Leg 156 Shipboard Science Party (1996) Strain decoupling across the decollement of the Barbados accretionary prism. Geology 24:127–130. doi:10.1130/0091-7613

Hrouda F (1982) Magnetic anisotropy of rocks and its application in geology and geophysics. Geophys Surv 5:37–82

Hrouda F (1991) Models of magnetic anisotropy variations in sedimentary thrust sheets. Tectonophysics 185:203–210

Hrouda F, Janak F (1976) The changes in shape of the magnetic susceptibility ellipsoid during progressive metamorphism and deformation. Tectonophysics 34:135–148

Ising G (1942) On the magnetic properties of varved clay. Arkiv for Matematik, Astronomi och Fysik 29A:1–37

Jayangondaperumal R, Dubey AK, Kumar BS, Wesnousky SK, Sangode SJ (2010) Magnetic fabrics indicating Late Quaternary seismicity in the Himalayan foothills. Int J Earth Sci 99:S265–S278. doi:10.1007/s00531-009-0494-5

Jelinek V (1981) Characterization of the magnetic fabrics of rocks. Tectonophysics 79:T63–T67

Kissel C, Barrier E, Laj C, Lee TQ (1986) Magnetic fabric in 'undeformed' marine clays from compressional zones. Tectonics 5:769–781

Lee TQ, Angelier J (2000) Tectonic significance of magnetic susceptibility fabrics in Plio-Quaternary mudstones of south-western foothills, Taiwan. Earth Planet Space 52:527–538

Levi S, Nabelek J, Yeats RS (2005) Paleomagnetism based limits on earthquake magnitudes in northwestern metropolitan Los Angeles, California, USA. Geology 33:401–404. doi:10.1130/G21190.1

Levi T, Weinberger R, Aifa T, Eyal Y, Marco S (2006) Earthquake-induced clastic dikes detected by anisotropy of magnetic susceptibility. Geology 34:69–72. doi:10.1130/G22001.1

Pares JM, van der Pluijm BA (2002) Evaluating magnetic lineations (AMS) in deformed rocks. Tectonophysics 350:283–298

Pares JM (2004) How deformed are weakly deformed mudrocks? Insights from magnetic anisotropy. In: Martin-Hernandez F, Aubourg C, Jackson M (eds) Magnetic fabrics: methods and applications, vol 238. Special Publication Geological Society of London, pp 191–203

Pares JM, van der Pluijm BA, Dinares-Turell J (1999) Evolution of magnetic fabrics during incipient deformation of mudrocks (Pyrenees, northern Spain). Tectonophysics 307:1–14

Robion P, Grelaud S, Frizon de Lamotte D (2007) Pre-folding magnetic fabrics in fold-and-thrust belts: why the apparent internal deformation of the sedimentary rocks from the Minervois Basin (NE Pyrenees, France) is so high compared to the Potwar Basin (SW Himalaya, Pakistan)? Sed Geol 196:181–200

Rochette P (1987) Magnetic susceptibility of the rock matrix related to magnetic fabric studies. J Struct Geol 9:1015–1020

Sagnotti L, Faccenna C, Funiciello R, Mattei M (1994) Magnetic fabric and structural setting of Plio-Pleistocene clayey units in an extensional regime: the Tyrrhenian margin of central Italy. J Struct Geol 16:1243–1257

Sagnotti L, Speranza F (1993) Magnetic fabric analysis of the Plio-Pleistocene clayey units of the Sant'Arcangelo Basin, southern Italy. Phys Earth Planet Inter 77:165–176

Sagnotti L, Speranza F, Winkler A, Mattei M, Funiciello R (1998) Magnetic fabric of clay sediments from the external northern Apennines (Italy). Phys Earth Planet Inter 105:73–93

Saint-Bezar B, Hebert RL, Aubourg C, Robion P, Swennen R, de Lamotte DF (2002) Magnetic fabric and petrographic investigation of hematite-bearing sandstones within ramp-related folds: examples from the South Atlas Front (Morocco). J Struct Geol 24:1507–1520

Schwehr K, Tauxe L (2003) Characterization of soft sediment deformation: detection of cryptoslumps using magnetic methods. Geology 31:203–206

Tarling DH, Hrouda F (1993) The magnetic anisotropy of rocks. Chapman & Hall, London 217 pp

Voight W, Kinoshita S (1907) Bestimmung absoluter Werte von Magnetiserungszahlen, inbesondere fur Kristalle. Annale der Physic 24:492–514

http://www.springer.com/978-3-319-05587-9

Understanding an Orogenic Belt
Structural Evolution of the Himalaya
Dubey, A.
2014, XVI, 401 p. 306 illus., 12 illus. in color., Hardcover
ISBN: 978-3-319-05587-9